

Region-specific cell grafting into cervical and lumbar spinal cord in rat: a qualitative and quantitative stereological study

Osamu Kakinohana^a, Dasa Cizkova^a, Zoltan Tomori^b, Eva Hedlund^c, Silvia Marsala^d,
Ole Isacson^c, Martin Marsala^{a,*}

^aAnesthesiology Research Laboratory, University of California, San Diego-0818, La Jolla, San Diego, CA 92093, USA

^bInstitute of Experimental Physics, Slovak Academy of Sciences, Slovakia

^cNeuroregeneration Laboratory, McLean Hospital, Harvard Medical School, Belmont, MA 02478, USA

^dDepartment of Pathology, University of California, San Diego, La Jolla, San Diego, CA 92093, USA

Received 8 April 2004; revised 24 June 2004; accepted 15 July 2004

Abstract

In the present study, we have characterized an atraumatic grafting technique which permits multiple, segmental, and lamina-specific injections into cervical or lumbar spinal cord. Cell injections were performed in spinally mounted rats of different ages and spinal cord size, using a micromanipulator and glass microcapillary connected to a digital microinjector. For grafting, we used human neuroteratoma (hNT) cells, BrdU-labeled rat spinal precursors or primary embryonic spinal cord neurons isolated from E14 spinal cord of the eGFP+ rat. Systematic quantification of grafted cells was performed using stereological principles of systematic random sampling and semi-automated optical Disector software. Volume reconstruction was performed using serial sections from grafted areas and custom-developed software (Ellipse) which permits “two reference points” semi-automated alignment of images, as well as volume reconstruction and calculation. By coupling these techniques, it is possible to achieve a relatively precise and atraumatic cell delivery into multiple spinal cord segments and specific spinal laminae. Consistency of the multiple grafts position in the targeted laminar areas was verified by a systematic volume reconstruction. Good survival of implanted cells for the three different cell lines used indicate that this grafting technique coupled with a systematic analysis of the individual grafting sites can represent a valuable implantation-analytical system.

© 2004 Elsevier Inc. All rights reserved.

Keywords: Spinal cord; Laminae-specific grafting; ALS; Ischemia; Paraplegia

Introduction

Cell replacement therapy, with the goal of re-establishing local neuronal circuitry and/or to potentiate local release of trophic factors, represents a promising therapeutical approach in the treatment of a variety of spinal neuronal disorders including spinal trauma, amyotrophic lateral sclerosis, spinal ischemia, or multiple sclerosis. An important element in these studies is the development of a grafting technique that allows multiple cell injections within selected

spinal segments and lamina-specific cell delivery. It is also important to be able to quantify the survival of grafted cells in a systematic fashion, as well as to re-construct the positions of the individual grafting sites with respect to persisting neuronal pools. These represent the key analytical approaches permitting objective assessment of cell transplantation therapies. While at present, a variety of transplantation techniques are used to deliver cells of interest into an affected spinal cord regions a refinement of these grafting techniques which would permit a region-specific (lamina-specific) cell delivery is required. Such an approach would result in a more effective therapeutical effect particularly in pathological states characterized by a multi-segmental and region-specific neuronal loss (such as amyotrophic lateral sclerosis (ALS) or spinal ischemia).

* Corresponding author. Anesthesiology Research Laboratory, University of California, San Diego, 0818, 9500 Gilman Drive, La Jolla, San Diego, CA 92093. Fax: +1 619 543 6070.

E-mail address: mmarsala@ucsd.edu (M. Marsala).

ALS is characterized by a progressive degeneration of ventral α -motoneurons, corresponding loss of motor function and in final stages of the disease by the loss of respiratory function (Delisle and Carpenter, 1984). Recently, a transgenic model of SOD1 mutant-mediated ALS was developed in mice (Morrison et al., 1998) and rats (Howland et al., 2002). These animal models demonstrate a time-dependent loss of ventral α -motoneurons localized in lumbosacral area followed later by loss of cervical α -motoneurons and corresponding loss of ambulatory function and respiratory failure. Transient spinal cord ischemia is a serious complication of aortic cross-clamp, that is, procedure required to replace aortic aneurysm (Svensson, 1997; Svensson et al., 1986). Depending on the duration and completeness of ischemic period, it can be clinically expressed as spastic or flaccid paraplegia (Taira and Marsala, 1996; Zivin and DeGirolami, 1980). Histopathological analysis of the spinal cords in animals with ischemic spasticity show a selective loss of small inhibitory neurons (but with persisting α -motoneurons) in lumbosacral segments. In contrast, animals with fully developed flaccid paraplegia show spinal pan-degenerative changes involving small interneurons and ventral α -motoneurons (Marsala et al., 1989, 1991; Tarlov, 1967). While the etiology of ALS and spinal ischemic injury is fundamentally different, the final histopathological changes characterized by a selective loss of specific neuronal pools is remarkably similar. These similarities are particularly relevant in the view of a development of neuronal replacement therapy, which will permit multi-segmental and lamina-specific delivery of cells of interest.

In general, current techniques of spinal cord cell grafting can be considered in several categories depending on the general surgical approach used (single or multiple laminectomies), spinal column immobilization as well as on the techniques of actual cell injections (i.e., stainless steel needles or glass capillaries). First, mice spinal cell injections have been accomplished following partial laminectomy of Th13 vertebra without spinal column immobilization using pulled-glass pipette (Hartley et al., 1999). Second, rat cervical or thoracic spinal cell delivery have been performed using glass microcapillary or 33 gauge needle attached to a Hamilton syringe (Blesch and Tuszynski, 2003; Giovanini et al., 1997; Schwartz et al., 2003) without spinal column immobilization. Third, spinally mounted pre-lesioned mice have been injected into thoracic spinal cord using a glass microcapillary (Cummings et al., 2003). Because of the nature of these studies, that is, the use of control animals or animals after localized spinal trauma, only limited number of injections (Basso et al., 1996; Blesch and Tuszynski, 2003; Cummings et al., 2003; Delisle and Carpenter, 1984; Dirig et al., 1997; Gao et al., 1998; Giovanini et al., 1997; Hargreaves et al., 1988; Hartley et al., 1999) were typically performed in these studies.

The goal of the present study using Sprague–Dawley (SD) rats was to develop a technique of spinal cell grafting,

which would (i) allow a consistent and well controlled cell delivery, (ii) permit a multi-segmental and lamina-specific cell injections, and (iii) will be atraumatic enough to have no effect on neurological function after multisegmental and bilateral cell grafting. Finally, an additional goal of this study was to develop a simple and easy-to-use image processing software which will permit (i) stereological cell counting using principles of unbiased systematic random sampling, (ii) an effective alignment of the stack of serial images taken from spinal cord coronal sections, (iii) calculation of the volume of interest in grafted areas, and (iv) subsequent 3-D reconstruction of multiple grafting sites.

Material and methods

Animals

Sprague–Dawley rats were obtained from Harlan (Indianapolis, USA). Transgenic rats, that express the human mutated form of SOD1, SOD1^{G93A}, and subsequently develop ALS, were obtained from Taconic (Germantown, MY). The transgenic “green rats” (“green rat CZ-004” SD TgN (act-EGFP)OsbCZ-004), in which eGFP is expressed from the actin promoter, a generous gift from Dr. Okabe (Osaka University, Japan), were bred at the animal facilities at UCSD. All animals were kept under controlled conditions of temperature and humidity and had free access to food and water. All animal procedures were performed according to protocols approved by Animal Subject Committee at University of California, San Diego.

General surgical preparations

Sprague–Dawley (SD) rats (200–400 g) were used in all grafting studies. In addition to control naive rats animals with spinal ischemic injury (Taira and Marsala, 1996) or rats expressing the human mutated SOD1^{G93A}, which develop ALS (Taconic) (Howland et al., 2002) were used (see Table 1 for experimental groups). In all cases, animals were anesthetized with halothane (2%) and paravertebral muscles overlaying either C4–C5 or L2–L5 vertebra were freed from the attachments. Animals were then mounted into a spinal unit (Stoelting, CO). Using a dental drill (ball style drill bits; 1 mm in diameter) partial laminectomy of C4 and C5 or L2–L5 vertebra was performed providing bilateral access to the left and the right dorsal horns (Fig. 1B). After cell grafting (see following paragraph), the wound was cleaned with 2% hydrogen peroxide followed by a mixture of penicillin/streptomycin and sutured in two layers using 5.0 silk.

Cell preparation

In the present study, three different cell lines were used for grafting. First, hNT neurons (Layton Biosciences, Inc, pre-treated with 5 μ M of retinoic acid for 14 days) previously

Table 1
Experimental groups

Experimental models*	Body weight (g)	Targeted area (segment/lamina)	Grafted cells**	Survival weeks
Control/naive (<i>n</i> = 12)	400 ± 22 or 180 ± 15	C4–C5/ Lamina IX L2–L5/ Lamina VII	hNT 16 bilateral injections	6–8 weeks
ALS (SOD-1) (<i>n</i> = 6)	220 ± 25	L2–L5/ Lamina IX	Embryonic primary neurons (green rat) 20–25 unilateral injections	7–8 weeks
Ischemic injury (<i>n</i> = 7)	350 ± 35	L2–L5/ Lamina VII	Spinal neuronal precursors (BrdU+) 40–50 bilateral injections	12 weeks

* In all groups immunosuppressive treatment (FK-506; 1 mg/kg/day) was used.

** In all cases, 15, 000–20, 000 cells were delivered per injection.

stored in liquid nitrogen were thawed at 37°C water bath and washed 2× in DMEM. hNT cells are a human embryonal carcinoma cell line derived from a teratocarcinoma (Andrews et al., 1984). Following retinoic acid treatment, these cells differentiate into pure postmitotic neurons (Lee and Andrews, 1986). Using electrophysiological and RT-PCR analysis, the presence of functional GABA and glutamate receptors (Neelands et al., 1998; Paterlini et al., 1998) as well as L- and N-type calcium channels has been demonstrated in these neurons (Gao et al., 1998). In addition, it has been shown that hNT neurons transcribe the glutamic acid decarboxylase p67 gene, suggesting their potential to develop an inhibitory phenotype (Yoshioka et al., 1997). Second, primary embryonic neurons were isolated from E14 rat lumbar spinal cord of “green rats”, using the Papain Dissociation System (Worthington Biochemical Corp., Freehold, New Jersey). Third, precursors were isolated from lumbar E14 spinal cord of SD rats and expanded in vitro for 10 days using EGF and FGF (10 ng/ml). Between 7 and 10 days after isolation, cells were labeled with BrdU (5 μM) for 24 h. After BrdU labeling, neuronal differentiation was induced with retinoic acid (1 μM) for 3 days in the absence of bFGF and EGF. The final cell concentration used for grafting was 15–20,000 cells/injection (0.5 μl) for all three cell lines used. Quantitative in vitro analysis of BrdU-labeled cells showed that on average 35–45% of cells were labeled with BrdU at 24 h after labeling.

Characterization of GFP+ cells in spinal cords of GFP+ rats

To identify the expression of GFP in different spinal neuronal pools of an adult eGFP+ rat animals (*n* = 4) taken from four different litters were perfusion fixed and spinal cord sections stained with NeuN antibody. In addition a primary E14 spinal cord (L1–L5 segments) culture was

prepared and cell cultured for 14–21 days using Nunclon 6 wells plate. Cells were fed with DMEM +5% FBS every 2–3 days. Cultures were then fixed with 4% paraformaldehyde and colocalization of GFP with neuronal (MAP2, NeuN; Chemicon 1:1000) and non-neuronal (GFAP-astrocyte marker; Sigma, 1:500; RIP-oligodendrocyte marker; Hybridoma Bank, Iowa, 1:1000) markers identified using a standard immunofluorescence techniques (see staining protocol).

Spinal cell grafting

To graft cells spinally, a glass microcapillary was prepared using a micropipette puller (Model M1; Industrial Science Assoc., Inc, NY). The tip of the capillary was then broken and polished with silicon carbide sand paper (size 320A). The diameter of the capillary tip was checked under microscope and only capillaries with the tip diameter of 80–100 μm were used in grafting studies (Fig. 1A). Before grafting, each capillary was flushed with 60% ethanol and left overnight under UV light (a standard Biosafety cabinet equipped with UV light was used). To ensure proper lamina-specific cell injections into lumbar and cervical spinal cord, measurements identifying the distance between the surface of the dorsal spinal cord and respective laminae (see Table 2) were made using transverse spinal cord sections taken from SD rats between 200 and 400 g of body weight. Using obtained coordinates, cells were injected into a specific spinal and laminar segments (see Table 1 for experimental groups). To ensure precise depth of injections, across all sites, as well as to simplify the use of the micromanipulator in between injections, a circular mark was made on the capillary at the specific distance from the capillary tip (i.e., depending on the previously measured depth of the targeted laminar area) using acetone-based black paint (Fig. 1A; arrow). A 30-gauge needle was used to apply the paint on the microcapillary. During injections, the capillary was advanced into spinal parenchyma so that the circular mark remained just above the spinal cord. All injections were made under visual control using an Olympus dissecting microscope (Model SZ-40). The patency of the capillary was checked after each single injection before proceeding to the next injection site. In all cases cells dispersed in DMEM were delivered in a volume of 0.5 μl during a 30-s interval. After each injection, the capillary was left in place for an additional 2 min. All grafted animals were immunosuppressed with 1 mg/kg/day Prograf (Tacrolimus capsules, Fujisawa Healthcare Inc, Deerfield, IL) with the treatment being initiated 3 days before transplantation and was maintained throughout the whole experiment.

Assessment of neurological function

In control and ALS rats motor and sensory functions were analyzed periodically before and in 7 days intervals after cell grafting. The motor functions was assessed using a

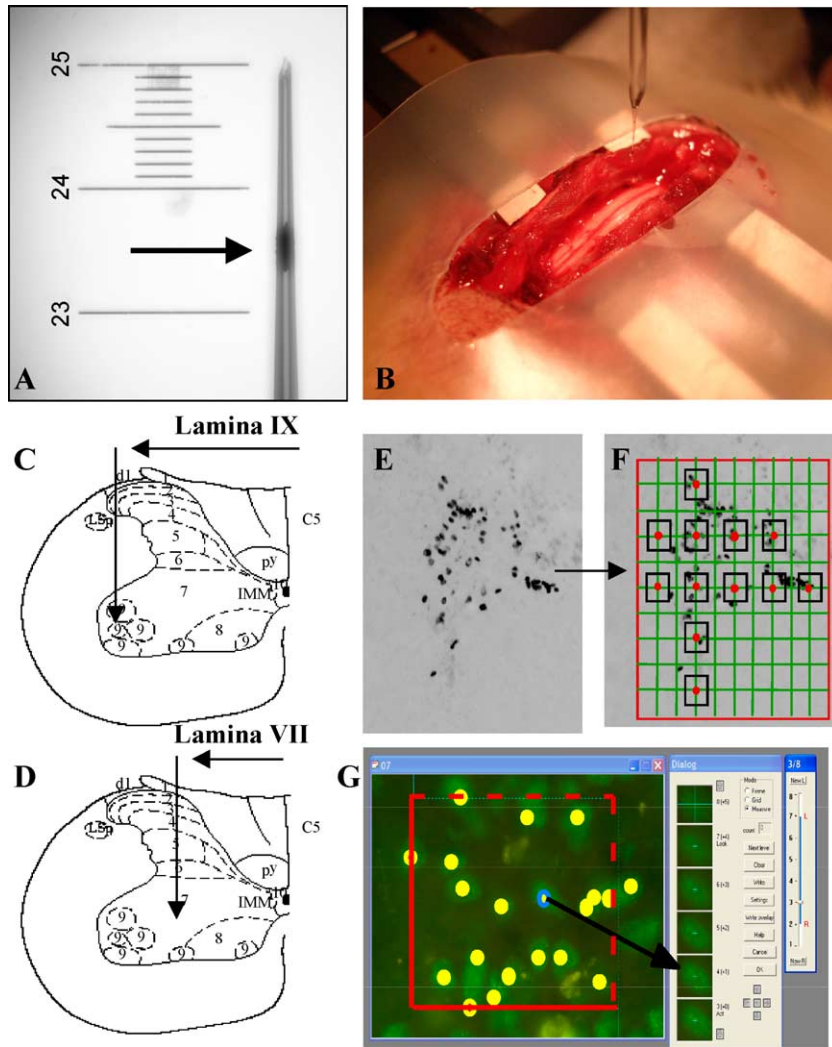


Fig. 1. (A) A glass microcapillaries were prepared using a micropipette puller and the tips were polished with a sand paper (see Materials and methods for details). A circular mark was made at a specific distance from the capillary tip using acetone-based back paint (A; arrow). (B) For cell grafting, animals are mounted into spinal attachment unit and multiple laminectomies performed using dental drill. (C, D) During injections, the capillary was advanced into the spinal parenchyma using previously measured coordinates for specific age/weight of animal, spinal segment as well as laminar region (i.e., lamina IX-C or lamina VII-D) (see Table 2 for details). (E–G) The total number of grafted cells was calculated from serial optical images taken from transverse spinal cord sections (30–40 μm thick) stained with nuclear antibody (NUMA or BrdU) after applying fractionator sampling scheme and using optical Disector software.

modified 21-point open field locomotor scale (Basso et al., 1996). BBB scores categorize combinations of rat hindlimb movements, trunk position and stability, stepping, coordination, paw placement, toe clearance, and tail position. Sensory functions were analyzed using three independent criteria: (i) reaction to hind paw (HP) pinch: 0 = normal

response; 1 = some response; and, 2 = no response. (ii) presence of allodynia: defined as a vigorous squeaking and agitation in response to light stroking of the flank, and (iii) thermal withdrawal threshold of the hind paw.

Thermal paw withdrawal was measured by placing the animals in Plexiglas cages (9 \times 22 \times 25 cm) on a modified

Table 2
Measured distances between the dorsal surface of the spinal cord and targeted LVII or LIX laminar regions

Weight(g)	C2		C5		L3		L4		L5	
	A/B (LVII)	A/B (LIX)	A/B (LVII)	A/B (LIX)	A/B (LVII)	A/B (LIX)	A/B (LVII)	A/B (LIX)	A/B (LVII)	A/B (LIX)
200	0.4/1.0	0.4/1.2	0.4/1.0	0.6/1.2	0.5/1.0	0.6/1.2	0.5/1.0	0.6/1.2	0.5/1.0	0.6/1.2
250	0.5/1.2	0.5/1.4	0.5/1.2	0.7/1.4	0.5/1.2	0.6/1.4	0.5/1.2	0.6/1.4	0.5/1.2	0.6/1.4
300	0.5/1.2	0.5/1.5	0.6/1.5	0.8/1.5	0.5/1.3	0.7/1.5	0.5/1.3	0.7/1.5	0.5/1.3	0.7/1.5
350	0.5/1.2	0.5/1.5	0.6/1.5	0.8/1.5	0.6/1.3	0.7/1.5	0.6/1.3	0.7/1.5	0.6/1.3	0.7/1.5
400	0.5/1.2	0.5/1.5	0.6/1.5	0.8/1.5	0.6/1.3	0.7/1.5	0.6/1.3	0.7/1.5	0.6/1.3	0.7/1.5

A: distance from midline in mm. B: depth from the dorsal surface in mm.

Hargreaves Box (Dirig et al., 1997; Hargreaves et al., 1988) (Department of Anesthesiology, University of California, San Diego, La Jolla, CA). This device consisted of a glass surface with a maintained surface temperature of 30°C. A stimulus lamp with a mirror attached to permit visualization of the under surface was focused on the plantar surface of the paw. An abrupt withdrawal of the hindpaw secondary to the 50°C stimulus was sensed by photodiodes, and this served to terminate the stimulus and stop the timer. To avoid tissue damage, failure to respond in 20 s automatically terminated the test (cut-off time) and this latency (20 s) was assigned. After a 20-min adaptation period, the first measurement was made on both hindpaws. The response latencies were averaged and assigned as the baseline score (time 0).

In addition, to the above tests the grip strength (the hanging wire test) was periodically measured in ALS rats. Each rat was placed on the wire-lid of a conventional housing cage. The lid was gently shaken to prompt the mouse to hold onto the grid before the lid was turned upside down. The latency until the rat let go with at least both hind limbs was timed. Each rat was given up to five attempts to hold on to the inverted lid for an arbitrary maximum of 90 s and the longest latency was recorded (Sango et al., 1996; Weydt et al., 2003).

Perfusion fixation and immunofluorescence staining

At the end of the survival periods (6–12 weeks), all animals were anesthetized with pentobarbital (40 mg/kg; i.p.) and phenytoin (25 mg/kg, i.p.) and transcardially perfused with saline for 1–2 min followed by 4% paraformaldehyde in 0.1M phosphate buffer (PB). Four hours after perfusion fixation, the spinal cords were removed and postfixed in the same fixative overnight at 4°C. After postfixation the tissue was cryoprotected in a graded sucrose solution (10%, 20%, and 30%). Frozen transverse spinal cord sections (20–30 µm) taken from L2–L5 segments were cut and collected on Fischer Plus slides. The slides were then placed into a 100% humidified chamber for 5 min and dried at RT to allow sufficient attachments of the sections to the glass surface. For immunocytochemical detection of BrdU, DNA was denatured to expose the antigen. Free-floating spinal cord sections were pretreated in 50% formamide-2× SSC at 65°C for 2 h and then incubated at 37°C for 30 min in 2N HCl. Sections were subsequently rinsed for 10 min at 25°C in 0.1 M boric acid (pH 8.5) and incubated with primary antibodies as described below.

All blocking and antibody steps were performed in 1× PBS/0.2% Triton-X (TX)/5% goat serum. Following 3 h, blocking sections were incubated with one of the following primary antibodies: rat anti-BrdU (1:200; Chemicon), NeuN antibody (1:1000; Chemicon), MOC (neural cell adhesion molecule; human specific; 1:250; Vector), the mitotic spindle protein NuMA (human-specific; 1:200; Chemicon)

for 72 h at 4°C. This was followed by PBS/TX wash (3 × 5 min) and incubation with secondary goat anti mouse antibody conjugated to a fluorescent marker (Alexa 488 or 594; 1:250; Molecular Probes) for 45 min at RT. For general nuclear staining DAPI (1:330) was added to the final secondary antibody solutions. In control experiments, primary antibodies were omitted. After staining, sections were dried at RT and covered by Prolong (Molecular Probes). Fluorescence slides were analyzed using a Leica Fluorescence microscope and captured using a digital camera (Hamamatsu-Orca-ER) or (Olympus; microfire; Model S99809). Overlaid images were prepared with Photoshop 7.0 (Adobe Systems, Mountain View, CA) and digitally stored for further processing.

Stereological quantification of grafted hNT neurons and SNPs and confocal microscopy

The total numbers of grafted neurons immunoreactive for the human nuclear (NUMA) or BrdU antibody were estimated using stereological, unbiased and systematic sampling (Figs. 1E–G) (Tomori et al., 2001; West, 1999; West et al., 1991). Frozen transverse spinal cord sections (30 µm thick) were cut in 100 µm intervals from L2–L5 or C4–C5 segments. Each tenth section was used for stereological quantification after applying the fractionator sampling scheme (Fig. 1F). The optical images (1 µm thick) were obtained by Leica DMLB microscope using immerse 100× oil objective with numerical aperture 1.3. The optical images were captured using a digital camera (Olympus) and ImagePro software (Media Cybernetics) supplied with a StagePro (Media Cybernetics) controlled motorized Z stage. The total number of grafted cells were calculated using the optical Disector software (Fig. 1G) and applying the fractionator formula $N = Q \times 1/hsf \times 1/asf \times 1/ssf$, where N is the total number of positive nuclei, Q is the sum of the cells counted, hsf is the height sampling fraction, asf is the area sampling fraction, and ssf is the slice sampling fraction.

3-D reconstructions and graft volume calculations

Previously stored images taken from serially cut spinal cords were used. On average, 60–100 serial sections were used for 3-D reconstruction and volume calculation of the individual grafting sites. In the first step, a stack of serial images was opened using Ellipse software and aligned using the custom developed Allign module (VidiTo, SK). The alignment process consisted of defining two morphological reference points in all serial spinal cord images (the first point: center of the central canal; the second point: medial border of the dorsal horn), and a subsequent computer-processed alignment of all images (Figs. 4A, B). To identify the borders of the dorsal and ventral horns, lines were then drawn on the stack of previously aligned images using Lamina Maps module (Ellipse) (Fig. 4C). Finally, the stack

of previously aligned and laminar maps-labeled images were used for 3-D reconstruction using 3-D constructor (Media Cybernetics) (Figs. 4D–I). The whole process of image alignment, laminar map labeling and 3-D reconstruction takes on average 20–30 min when 70–80 images are processed.

For volume calculation, a stack of previously aligned images were used. Images were opened in Ellipse software and the volume calculated using the Volume module. The whole process consisted of (i) defining the calibration parameters (X – Y and X – Z), and (ii) drawing the borders of the grafts on each image. The final analysis provides a sum of calculated volumes from all images used and a 3-D view of the previously outlined area in the stack of images (Figs. 5A, B, C, D).

Statistical analysis

For the statistical analysis of neurologic outcome, non-parametric tests were used. The overall treatment and time-dependent main effect was analyzed using Kruskal–Wallis test. Intergroup differences at a specific time points after grafting were analyzed using Mann–Whitney U test (an unpaired two-group test). P value of <0.05 was considered significant.

Results

Lumbar versus cervical cell grafting

In general, there were no technical difficulties with respect to cell delivery. The flow of the cell suspension across the capillary tip was readily identified during each injection. If the flow was not detected, the capillary was pulled out and retested. Usually, in these cases, a small piece of tissue was found in the tip of the capillary and was then removed using a saline-soaked cotton swab. On average, 8–16 injections were made bilaterally between C4 and C5 spinal segments or 20–50 injections between L2 and L5 segments. Two out of three animals with a body weight of 180 ± 15 g died during the first hour after bilateral C4–C5 grafting. Animals with body weights of 400 ± 22 g and receiving cervical grafts as well as all animals, which received lumbar grafts showed no detectable side effect immediately after injections or during recovery from anesthesia. Anatomical analysis of all animals with long-term surviving grafts showed no or minimal fibrotic changes at the injections sites after perfusion.

Neurological assessment

In control or in ALS grafted rats, no significant changes in ambulatory motor functions (BBB score) were seen if compared before and 1–4 weeks after grafting. Similarly no detectable sensory deficit or presence of allodynia was

seen at any post-grafting time point. Baseline thermal withdrawal threshold was 12 ± 2 s and was 11 ± 3 between 1 and 4 weeks after cell injections. No significant differences were detected. In ALS rats the baseline grip test time was 35 ± 17 s. There were no significant differences recorded between 1 and 4 weeks after grafting (i.e., during pre-symptomatic period) if compared to baseline.

Expression of green fluorescence protein in spinal cord of GFP+ rats

Transverse spinal cord sections cut from lumbar spinal cord of a GFP+ rat and stained with NeuN antibody showed that the majority of NeuN-positive small neurons in the dorsal horn were GFP negative (Figs. 2A, B, C; arrow). Only a weak GFP fluorescence was seen in some large interneurons and α -motoneurons in the ventral horn (Fig. 2D, E, F; arrows). However, similarly as seen in dorsal horn, a completely GFP-negative NeuN-positive neurons were also identified in the ventral horn (Fig. 2G; arrow). Staining of primary spinal cord culture with MAP2 antibody confirmed that the majority of MAP2-positive neurons were GFP-negative (Figs. 2J, K, L). In contrast, staining with GFAP antibody (Figs. 2M, N, O) or RIP antibody (Figs. 2P, R, S) showed an intense green fluorescence particularly identified in cell nuclei.

Laminar localization and quantification of grafted cells

Histological examination of the grafts showed that the majority of the cells were localized in the laminar areas targeted by the surgery. Thus, in control animals, after cervical grafting of hNT neurons, the epicenter of the graft was identified in lamina IX (Figs. 3A, B, C). General identification of the borders of the grafts was performed using membrane-bound MOC immunofluorescence staining (Fig. 3A), while identification of the individual hNT neurons was achieved using human specific nuclear (NuMA) staining (Fig. 3B).

Grafting of the spinal cord using primary spinal cord neurons isolated from the green rat into the SOD1^{G93A} rat lumbar spinal cord gave a similar distribution pattern to that seen in control rats. Grafts were easily identified in the lateral part of the ventral horn by the presence of green fluorescence (Fig. 3D) and the existence of grafted neurons was confirmed by immunofluorescence staining for NeuN (Figs. 3E, F). Double labeling of GFP-positive grafts showed a clear GAD65 (Fig. 4J), synaptophysin (Fig. 4K) as well as MAP2 (Fig. 4L) immunoreactivity within the graft. In ischemic animals with the cells grafted into the intermediate zone (lamina VII), the core of the individual BrdU-positive grafts were identified in the central gray matter (Fig. 3G). Numerous BrdU-positive cells showed colocalization with NeuN immunoreactivity (Figs. 3H, I). Both after cervical and lumbar

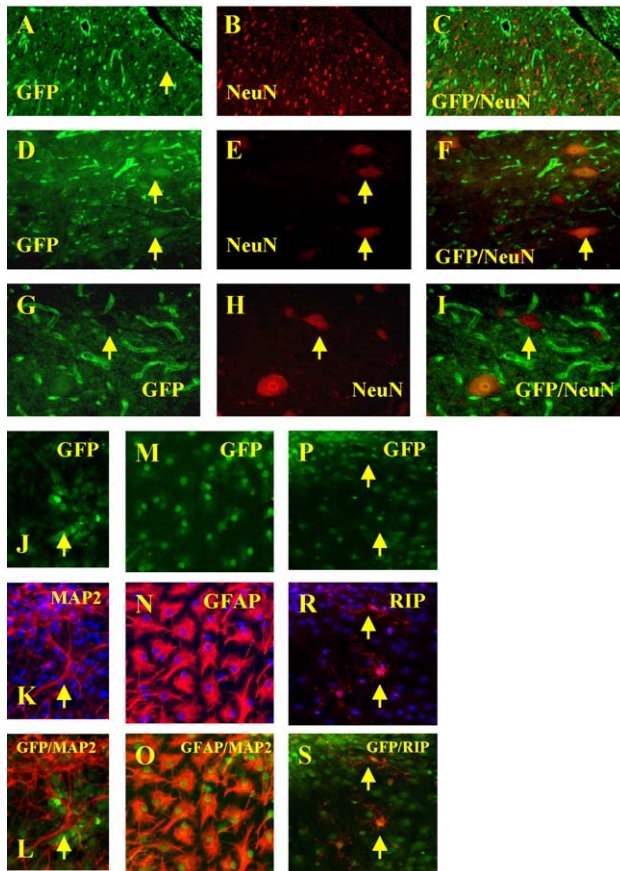


Fig. 2. (A–I) NeuN staining of transverse lumbar spinal cord sections taken from a GFP + transgenic rat. The majority of small dorsal horn neurons (A; arrow) and some large interneurons (G; arrow) are GFP-negative. Only some α -motoneurons showed a modest GFP positivity (D, E, F; arrows). (J–S) Primary spinal cord culture isolated from E14 GFP+ rat embryonic lumbar spinal cords and cultured for 21 days in DMEM+ 5% FBS. Double staining with MAP2 antibody show lack of GFP positivity in MAP2-positive neurons (J, K, L; arrow). In contrast, an intense green fluorescence expression primarily seen in nuclei of cultured GFAP-positive astrocytes (M, N, O) and RIP-positive oligodendrocytes (P, R, S; arrow) was detected.

cell delivery, a residue of grafted cells was identified along the needle tract from the surface of the dorsal horn toward the targeted areas.

Subsequent 3-D reconstruction prepared from serial sections showed consistent placement and distribution between individual grafted sites across animals. In control animals receiving cervical injections of hNT neurons at a distance of $>300 \mu\text{m}$ between individual graft sites, gaps of host tissue were easily identified (Figs. 4D, E). In animals grafted with primary embryonic spinal cord neurons isolated from green rats, the distance between individual injections was less, 200–300 μm . In this case, a homogeneous GFP-positive structure representing a composition of several grafts was typically seen (Figs. 4F–I). 3-D reconstruction of cervical spinal cord serial sections confirmed the reproducibility of spinal graft placement across sites and animals.

Stereological quantification of grafted cells and volume calculation of the individual grafting site

Systematic stereological quantification of grafted hNT or BrdU-labeled neurons showed on average 6–12% survival in the individual grafting sites (Table 3). Calculation of the volumes of the individual grafting sites showed on average $160,000 \pm 45,000 \mu\text{m}^3$ per grafting sites (Figs. 5A, B, C, D).

Discussion

Strategy for cell replacement therapy in ALS and spinal ischemic injury

In the present study, based on laminar and segmental distribution of neuronal loss seen in SOD1^{G93A} rats or in rats with spinal ischemic injury, two different segmental (cervical and lumbar) and laminar (intermediate zone or ventral horns) areas were targeted for cell grafting. After spinal ischemia, there is a selective loss of small inhibitory neurons in lumbo-sacral segments and this loss is fully developed (mature) 2–4 days after ischemia. A similar quantitative and qualitative histopathological picture has been described in several animal models of transient spinal ischemia as well as in human (Svensson et al., 1986; Taira and Marsala, 1996; Tarlov, 1967; Zivin and DeGirolami, 1980). After this peri-acute posts ischemic period, despite near complete or complete loss of ambulatory function, animals can survive for a prolonged period of time (more than 1 year). Even in these chronic stages of ischemic paraplegia, there is a continuing presence of lumbar α -motoneurons and no further deterioration in spinal pathology is seen. These characteristics of spinal ischemic injury (i.e., well-defined time frame of spinal neuronal degeneration and selective loss of inhibitory neurons in specific spinal segments and laminar regions) provide a near-optimal and clinically relevant model for cell replacement therapy. Importantly, cell grafts are targeted into areas that are characterized by fully developed neuronal loss and therefore the risk associated with injection itself and resulting mechanical injury to persisting neurons of the host are minimal. So far, we have grafted more than 130 animals with chronic ischemic spasticity with the average number of bilateral grafts localized between L2 and L5 being 35–40. No detectable side effect such as progression from spasticity to flaccidity (indicative of injection-related α -motoneuronal injury) or bladder dysfunction was seen in these animals.

In contrast to spinal ischemia, the time course as well as the corresponding physiological effects of neuronal degeneration in ALS is quite different. In the SOD1^{G93A} ALS transgenic rat model the expected life span is approximately 120 days. Clearly identified signs of neurological deterioration can be seen from day 90 to 100 and are initially characterized by loss of motor tone in lower extremities, corresponding to loss of peripheral myogenic

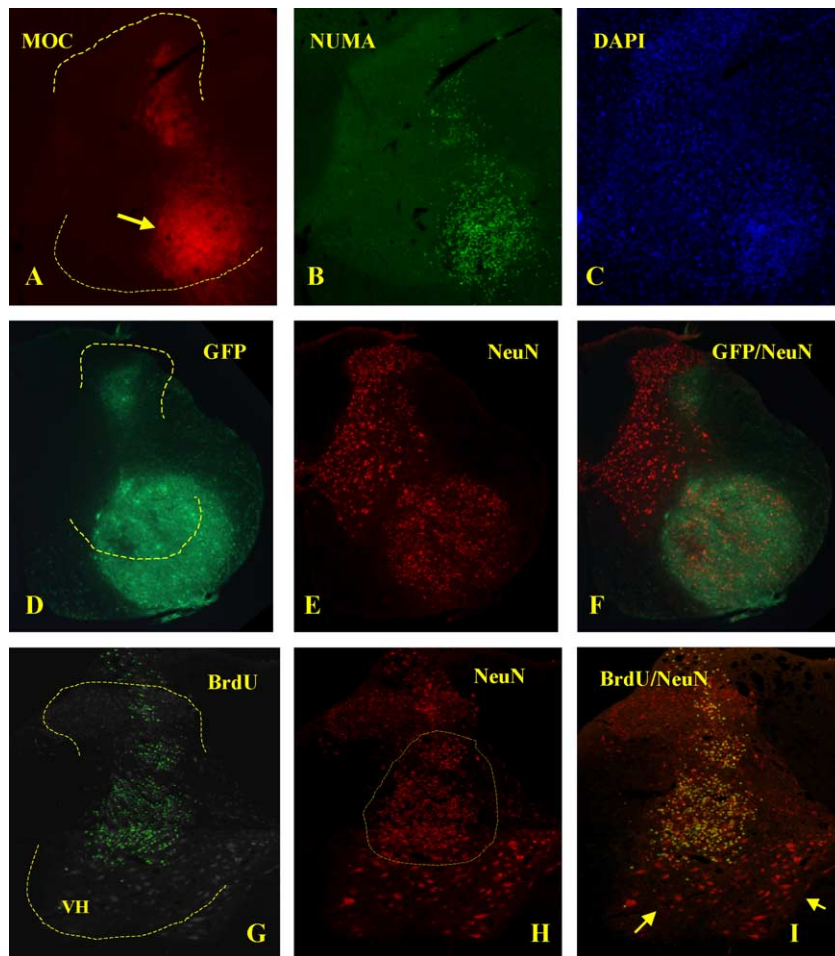


Fig. 3. (A, B, C) Human hNT neurons grafted into lateral part of the ventral horn of C3 spinal segment and stained with human specific MOC (A) and NUMA (B) antibody. The majority of grafted cells in the targeted area (lamina IX) can be seen (A; arrow). (D, E, F) Rat spinal cord embryonic primary neurons isolated from green rat and grafted into lumbar spinal cord (L3–4) of ALS rat. A GFP-positive graft in the lateral aspect of the ventral horn can be identified. Numerous NeuN-positive neurons in the core of GFP+ graft can also be seen (E, F: red). (G, H, I) BrdU-labeled rat spinal neural precursors grafted into intermediate zone in SD rats after spinal ischemic injury. The majority of BrdU-positive cells that colocalize with NeuN immunoreactivity in the central gray matter (lamina VII) can be seen (G; BrdU staining-green fluorescence; H; NeuN-red). Note a continuing presence of medial and lateral groups of α -motoneurons (I; bilateral arrows).

motor-evoked potentials and followed later by respiratory failure. Histopathological analysis of the spinal cord shows significant loss of ventral α -motoneurons localized in both lateral and medial group (Howland et al., 2002). Based on these characteristics, the grafting strategy will likely require cell transplantation into both cervical and lumbar ventral horns and will need to be performed during pre-symptomatic period (i.e., period of continuing and functional presence of the host α -motoneurons). This represents a significant challenge from the perspective of a grafting strategy and safety in ALS models. As demonstrated in the present study, bilateral (eight injections on both sides) cervical injections of hNT neurons lead to respiratory failure in two out of three animals with body weight of 180 g when injections were distributed bilaterally between C4 and C5 spinal segments. The size of these animals (7–8 weeks) corresponds to pre-symptomatic SOD1^{G93A} rats. We believe that the mechanism of this failure is related to

a transient depolarization of local α -motoneurons resulting from local tissue expansion at the injection sites (even though only 0.5 μ l was used per injection site). While not defined in the present study, we speculate that transient postoperative artificial ventilation will be necessary to permit a bilateral cell grafting into C4–C5 segments if performed in this age and body weight. Alternatively, cervical grafting can be performed in two separate grafting sessions, one targeted to the left and the second to the right site of C4–C5 segments.

Stereological quantification and volume/3-D reconstruction in spinal grafting studies

Using stereological quantification of grafted cells, an average of 6–12% of cell survival was detected in the individual grafting sites for both BrdU-labeled spinal precursors and hNT neurons. These numbers are similar to

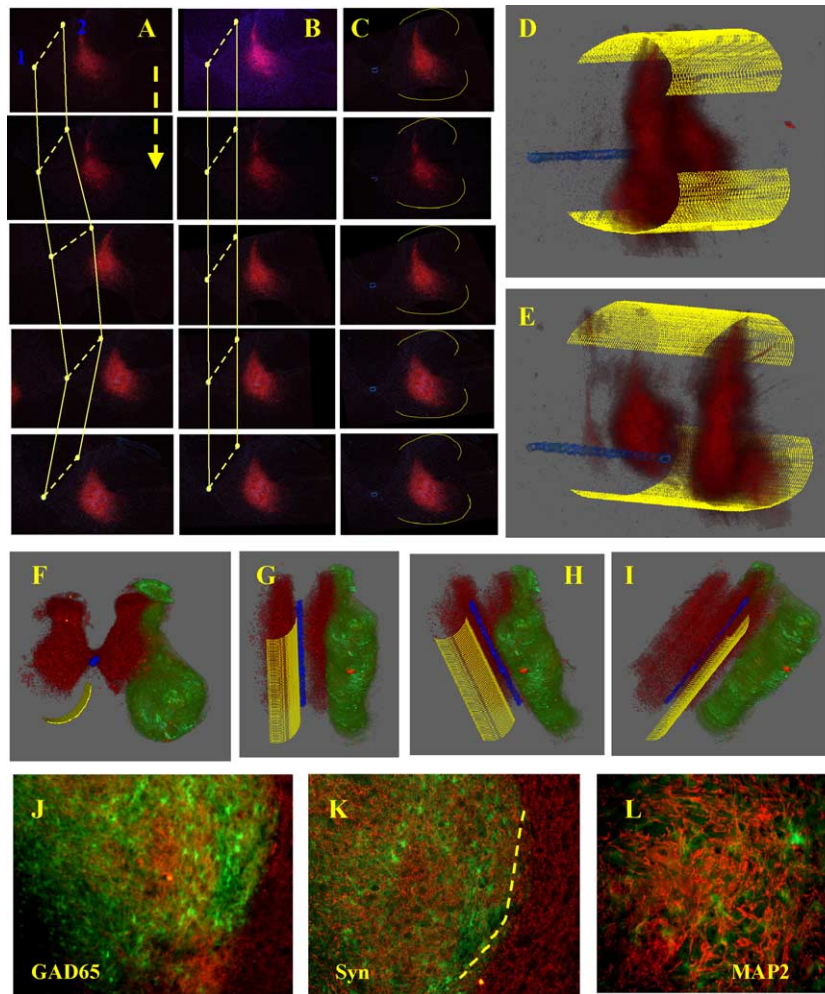


Fig. 4. (A, B, C) A stack of serial images with identified grafts is aligned using two reference points align system and semi-automated computer control image analysis software (Ellipse). The first reference point was always at the center of the central canal (identified from DAPI staining), (A; number 1) and the second one at the medial border of the dorsal horn (A; number 2). After alignment, the external borders of the dorsal and ventral horns were drawn on all images (C; yellow dashed lines). (D, E) Previously aligned images taken from an animal grafted with human hNT neurons in C4–C5 segments were used for 3-D reconstruction. Note a proper localization of two grafting sites in the lateral part of the ventral horn (grafts-MOC staining-red; central canal-blue). (F–I) Several views of 3-D reconstructed spinal cord depicting three individual grafting sites in an ALS animal which received green rat embryonic spinal cord neurons. Note the presence of a homogenous GFP-positive structure localized in the ventro-lateral part of the lumbar gray matter. (J, K, L) Double labeling of GFP+ grafts showed a clear GAD65 (J), synaptophysin (K) and MAP2 (L) immunoreactivity with the grafts.

numbers published from other laboratories after spinal grafting (Hartley et al., 1999; Saporta et al., 2001). In both cases, nuclear markers (NuMA or BrdU immunofluorescence staining) were used to identify grafted cells for stereological counting. In more recent studies, we have used lentivirus-labeled (Syn-EGFP) spinal progenitors for grafting. Although this labeling technique does not provide nuclear identification of labeled neurons, it is sufficient to identify individual grafted neurons from a series of optical

images (unpublished observation) when used in combination with DAPI staining. For 3-D reconstruction and volume calculations, custom-developed software (Align) was used which permitted semi-automated alignment of a stack of images. On average, 50–200 serial images (taken from 20 to 30 μm thick sections) were used for subsequent 3-D reconstructions. As demonstrated, the number of images used provides sufficient spatial resolution to identify individual grafts. In addition, in combination with double

Table 3

Stereological quantification of hNT neurons and BrdU-labeled rat neuronal precursors at 8–12 weeks after grafting

Animal no	1 (hNT)	2 (hNT)	3 (hNT)	4 (hNT)	1 (BrdU)	2 (BrdU)	3 (BrdU)	4 (BrdU)	5 (BrdU)
No. of grafts analyzed	7	8	8	10	6	7	7	8	9
Total cell counts	176,000	96,000	120,000	182,000	117,000	138,000	121,000	147,000	149,000
\pm	9000	13,000	11,000	800	22,000	24,000	34,000	29,000	37,000

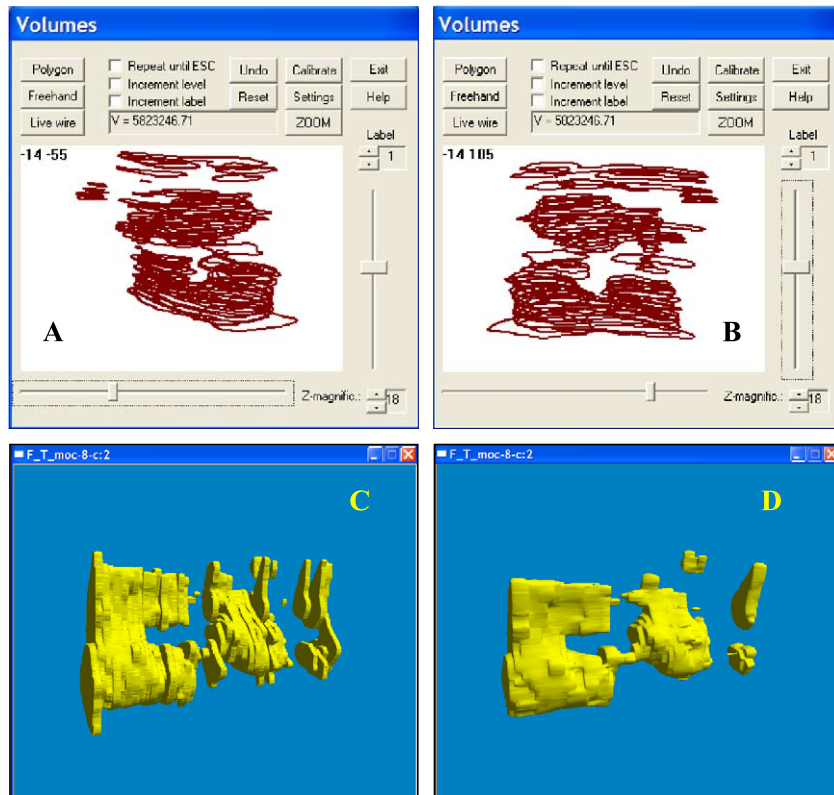


Fig. 5. (A–D) To calculate the volume of the individual grafts (also shown in Figs. 4D, E) a border of the graft was marked using a “freehand” drawing function on each serial section and the volume calculated. Calculated areas as well as individual grafts can be easily identified (A and B). C and D represent 3-D reconstructions (Ellipse) of two grafting sites shown in A and B. In D, a “smooth” function was applied.

or triple fluorescence-stained sections that separate the host neurons from grafted cells, detailed information on the vicinity grafted cells vs. host cells was obtained. Technically, the same image processing system (i.e., alignment of a stack of images as well as 3-D reconstruction and volume calculation) can be used with any serially prepared images in which two reference points can be identified (for example coronal or sagittal brain sections).

Experimental use of precursor cells and primary embryonic spinal cord neurons isolated from green rat

As demonstrated, the majority of spinal cord neurons in an adult green rat were GFP negative. Only some α -motoneurons expressed relatively weak green fluorescence. This observation was then confirmed in vitro by demonstrating a lack of GFP expression in MAP2-positive neurons. In contrast, astrocytes and oligodendrocytes showed high GFP expression seen particularly in nuclei. These data demonstrate that to analyze objectively, the proportion of grafted neurons derived from green rat precursors will require a systematic quantitative analysis (grafted vs. non-grafted animals) and combined staining of grafted cells/neurons with other neuronal markers such as NeuN. However, an intense GFP expression in glial cells appears to provide a clear advantage in easy identification of the individual grafts.

Conclusions

In the present study, we provide a technical description of a spinal grafting technique used for multiple segmental and laminar cell transplantation. This technique is then coupled with a systematic stereological quantification of grafted cells as well as 3-D reconstruction and volume calculations of multiple grafting sites. Data obtained in these studies demonstrate that this grafting technique and subsequent analytical approach in combination with behavioral assessment can provide an objective tool to validate a possible treatment effect resulting from a region-specific cell grafting in several models of spinal neuronal degeneration including ALS, spinal ischemia, and trauma.

Acknowledgments

Work was supported by ALSA (OI and MM), Slovak Grant agency (Grant No: 4068-Z.T.), NIH-NS 40386 (M.M) and Swedish Brain Foundation (EH).

References

Andrews, P.W., Damjanov, I., Simon, D., Banting, G.S., Carlin, C., Dracopoli, N.C., Føgh, J., 1984. Pluripotent embryonal carcinoma

- clones derived from the human teratocarcinoma cell line Tera-2. Differentiation *in vivo* and *in vitro*. *Lab. Invest.* 50, 147–162.
- Basso, D.M., Beattie, M.S., Bresnahan, J.C., Anderson, D.K., Faden, A.I., Gruner, J.A., Holford, T.R., Hsu, C.Y., Noble, L.J., Nockels, R., Perot, P.L., Salzman, S.K., Young, W., 1996. MASIS evaluation of open field locomotor scores: effects of experience and teamwork on reliability. Multicenter Animal Spinal Cord Injury Study. *J. Neurotrauma* 13, 343–359.
- Blesch, A., Tuszynski, M.H., 2003. Cellular GDNF delivery promotes growth of motor and dorsal column sensory axons after partial and complete spinal cord transections and induces remyelination. *J. Comp. Neurol.* 467, 403–417.
- Cummings, B.J., Uchida, N., Salazar, D.L., Tamaki, S.J., Dohse, M., Tushinski, R., Tsukamoto, A.S., Anderson, A.J., 2003. Transplantation of human central nervous system stem cells into a NOD-SCID mouse model of spinal cord contusion injury. *Soc. Neurosci. (Abstracts)* 415. 3.
- Delisle, M.B., Carpenter, S., 1984. Neurofibrillary axonal swellings and amyotrophic lateral sclerosis. *J. Neurol. Sci.* 63, 241–250.
- Dirig, D.M., Salami, A., Rathbun, M.L., Ozaki, G.T., Yaksh, T.L., 1997. Characterization of variables defining hindpaw withdrawal latency evoked by radiant thermal stimuli. *J. Neurosci. Methods* 76, 183–191.
- Gao, Z.Y., Xu, G., Stwora-Wojczyk, M.M., Matschinsky, F.M., Lee, V.M., Wolf, B.A., 1998. Retinoic acid induction of calcium channel expression in human NT2N neurons. *Biochem. Biophys. Res. Commun.* 247, 407–413.
- Giovanini, M.A., Reier, P.J., Eskin, T.A., Wirth, E., Anderson, D.K., 1997. Characteristics of human fetal spinal cord grafts in the adult rat spinal cord: influences of lesion and grafting conditions. *Exp. Neurol.* 148, 523–543.
- Hargreaves, K., Dubner, R., Brown, F., Flores, C., Joris, J., 1988. A new and sensitive method for measuring thermal nociception in cutaneous hyperalgesia. *Pain* 32, 77–88.
- Hartley, R.S., Trojanowski, J.Q., Lee, V.M., 1999. Differential effects of spinal cord gray and white matter on process outgrowth from grafted human NTERA2 neurons (NT2N, hNT). *J. Comp. Neurol.* 415, 404–418.
- Howland, D.S., Liu, J., She, Y., Goad, B., Maragakis, N.J., Kim, B., Erickson, J., Kulik, J., DeVito, L., Psaltis, G., DeGennaro, L.J., Cleveland, D.W., Rothstein, J.D., 2002. Focal loss of the glutamate transporter EAAT2 in a transgenic rat model of SOD1 mutant-mediated amyotrophic lateral sclerosis (ALS). *Proc Natl Acad Sci. U. S. A.* 99, 1604–1609.
- Lee, V.M., Andrews, P.W., 1986. Differentiation of NTERA-2 clonal human embryonal carcinoma cells into neurons involves the induction of all three neurofilament proteins. *J. Neurosci.* 6, 514–521.
- Marsala, J., Sulla, I., Santa, M., Marsala, M., Mechírová, E., Jalc, P., 1989. Early neurohistopathological changes of canine lumbosacral spinal cord segments in ischemia–reperfusion-induced paraplegia. *Neurosci. Lett.* 106, 83–88.
- Marsala, J., Sulla, I., Santa, M., Marsala, M., Zacharias, L., Radonak, J., 1991. Mapping of the canine lumbosacral spinal cord neurons by Nauta method at the end of the early phase of paraplegia induced by ischemia and reperfusion. *Neuroscience* 45, 479–494.
- Morrison, B.M., Janssen, W.G., Gordon, J.W., Morrison, J.H., 1998. Time course of neuropathology in the spinal cord of G86R superoxide dismutase transgenic mice. *J. Comp. Neurol.* 391, 64–77.
- Neelands, T.R., Greenfield Jr., L.J., Zhang, J., Turner, R.S., Macdonald, R.L., 1998. GABAA receptor pharmacology and subtype mRNA expression in human neuronal NT2-N cells. *J. Neurosci.* 18, 4993–5007.
- Paterlini, M., Valerio, A., Baruzzi, F., Memo, M., Spano, P.F., 1998. Opposing regulation of tau protein levels by ionotropic and metabotropic glutamate receptors in human NT2 neurons. *Neurosci. Lett.* 243, 77–80.
- Sango, K., McDonald, M.P., Crawley, J.N., Mack, M.L., Tiffit, C.J., Skop, E., Starr, C.M., Hoffmann, A., Sandhoff, K., Suzuki, K., Proia, R.L., 1996. Mice lacking both subunits of lysosomal beta-hexosaminidase display gangliosidosis and mucopolysaccharidosis. *Nat. Genet.* 14, 348–352.
- Saporta, S., Willing, A.E., Zigova, T., Daadi, M.M., Sanberg, P.R., 2001. Comparison of calcium-binding proteins expressed in cultured hNT neurons and hNT neurons transplanted into the rat striatum. *Exp. Neurol.* 167, 252–259.
- Schwartz, E.D., Shumsky, J.S., Wehrli, S., Tessler, A., Murray, M., Hackney, D.B., 2003. *Ex vivo* MR determined apparent diffusion coefficients correlate with motor recovery mediated by intraspinal transplants of fibroblasts genetically modified to express BDNF. *Exp. Neurol.* 182, 49–63.
- Svensson, L.G., 1997. New and future approaches for spinal cord protection. *Semin. Thorac. Cardiovasc. Surg.* 9, 206–221.
- Svensson, L.G., Von Ritter, C.M., Groeneveld, H.T., Rickards, E.S., Hunter, S., Robinson, M.F., Hinder, R.A., 1986. Cross-clamping of the thoracic aorta. Influence of aortic shunts, laminectomy, papaverine, calcium channel blocker, allopurinol, and superoxide dismutase on spinal cord blood flow and paraplegia in baboons. *Ann. Surg.* 204, 38–47.
- Taira, Y., Marsala, M., 1996. Effect of proximal arterial perfusion pressure on function, spinal cord blood flow, and histopathologic changes after increasing intervals of aortic occlusion in the rat [see comments]. *Stroke* 27, 1850–1858.
- Tarlov, I.M., 1967. Rigidity in man due to spinal interneuron loss. *Arch. Neurol.* 16, 536–543.
- Tomori, Z., Kubinova, L., Krekule, I., 2001. Disector program for unbiased estimation of particle number, numerical density and mean volume. *Image Anal. Stereol.* 20, 119–130.
- West, M.J., 1999. Stereological methods for estimating the total number of neurons and synapses: issues of precision and bias. *Trends Neurosci.* 22, 51–61.
- West, M.J., Slomianka, L., Gundersen, H.J., 1991. Unbiased stereological estimation of the total number of neurons in the subdivisions of the rat hippocampus using the optical fractionator. *Anat. Rec.* 231, 482–497.
- Weydt, P., Hong, S.Y., Klotz, M., Moller, T., 2003. Assessing disease onset and progression in the SOD1 mouse model of ALS. *NeuroReport* 14, 1051–1054.
- Yoshioka, A., Yudkoff, M., Pleasure, D., 1997. Expression of glutamic acid decarboxylase during human neuronal differentiation: studies using the NTERA-2 culture system. *Brain Res.* 767, 333–339.
- Zivin, J.A., DeGirolami, U., 1980. Spinal cord infarction: a highly reproducible stroke model. *Stroke* 11, 200–202.